CONTINUUM DAMAGE MECHANICS MODEL AS AN INSTRUMENT FOR DEVELOPMENT OF DESIGN RULES FOR STEEL STRUCTURES IN SEISMIC AFFECTED ZONES

B. HOPPE[*], Y. DI[*], D. NOVOKSHANOV[*], S. MÜNSTERMANN[*]

[*] Department of Ferrous Metallurgy (IEHK)
RWTH Aachen University
Intzestrasse 1, 52072 Aachen, Germany
e-mail: barbara.hoppe@iehk.rwth-aachen.de, www.iehk.rwth-aachen.de

Key words: Coupled Damage Mechanics Model, ULCF, HSLA Steel, Toughness Properties.

1 INTRODUCTION

Modern HSLA steels show a superior profile in mechanical properties as they have a high yield strength as well as excellent toughness properties. Nevertheless, HSLA steels are still only rarely used for steels constructions despite their excellent property balance of strength and toughness. This rare application is due to the fact that there are no reliable quantitative methods to predict damage initiation in HSLA steels components; hence, there is not yet a conclusive limit state analysis for components. One criterion of such a limit state analysis should be a consideration how steels components react under external loading influence like cyclic loading with large strain amplitudes as they occur during seismic events. Conventional, well established fracture mechanics approaches are unfit for the description of phenomenological occurrences under ULCF loading since they do not consider the ongoing kinematic hardening conditions and the J-integral is not applicable for cyclic loading conditions with large plastic strain amplitudes.

Thus, the material properties to consider are toughness and stiffness. To get a better understanding of their influence and relationship onto each other an examination through a coupled damage mechanics approach might be helpful. Over the years scientists developed many different approaches to encounter this issue. A macroscopic approach was proposed by Gurson [8] and led to a family of similar models. Another strategy was chosen by the limit strain concept most famously encountered by Bai and Wierzbicki [3]. Later on then modified with Lode-angle consideration by Lian et al. [1], the so called modified Bai − Wierzbicki (MBW) model. Also, there have been many different propositions made to encounter the issue of cyclic loading. Most known would be the model introduced by Armstrong and Frederick [2] with its non-linear kinematic hardening law. Other more advanced models came from Chaboche [6] or also, the two yield surface approach by Yoshida and Uemori [5].

As previously discussed, damage mechanics approaches are able to give a limit state analysis because of a local strain approach. Nevertheless, as it becomes obvious from the previous state of the art representation, some modifications need to be done to a general damage mechanics approach Such an approach was done in this paper. The modified Bai-Wierzbicki

model as provided by Lian [1] is a coupled damage model that has proven to give good results for state limit analysis for modern steels under monotonic load. Since it is assumed that the onset of damage is not different under monotonic or cyclic loading, in the frame of this work, the MBW model was used as foundation for the model regarding damage initiation and evolution. Armstrong-Frederick provided a good plasticity model to depict material behaviour cyclic loading conditions. It was used to replace the plasticity core of the MBW model. The damage evolution also considers an effective strain concept.

For the experimental part of this work, the focus lies on the ductile damage crack criterion based on the model by Lian and the parameter calibration to find the damage initiation locus. In a following step a possibility for a toughness criterion is proposed based on nominal damage initiation curves.

2 COUPLED DAMAGE MECHANICS MODEL FOR ULCF

There hereby presented plasticity model consists of a plasticity core based on the Armstrong-Frederick model [2] with a non-linear kinematic hardening law to depict the hardening and softening effects during cyclic loading and a ductile crack initiation criterion with a corresponding damage evolution law following the modified Bai-Wierzbicki model proposed by Lian [1].

2.1 Plasticity core based on Armstrong-Frederick model

The plasticity model chosen to depict mechanic effects that occur under cyclic loading conditions such as the Bauschinger effect is the Armstrong-Frederick model [2]. The aim is to reproduce local stress and strain features of the material in detail. In equation (1) the equation to describe the von Mises yield surface can be seen. In the genuine Armstrong- Frederick model the size of the yield surface was considered to be constant. In this version of the model this condition was relaxed by the term $k^2(\varepsilon_q)$.

$$F = \frac{1}{2}(\boldsymbol{s} - \boldsymbol{a}) \cdot (\boldsymbol{s} - \boldsymbol{a}) - \frac{k^2(\varepsilon_q)}{3} = 0 \tag{1}$$

The yield surface can now change in size depending on the amount of equivalent plastic strain. Therefore, the hardening of the material can consequently be considered as mixed isotropic-kinematic.

$$\dot{\boldsymbol{a}} = C(\varepsilon_{qpl})\dot{\boldsymbol{\varepsilon}}^p - \gamma\boldsymbol{\alpha}\dot{\varepsilon}_q \tag{2}$$

The kinematic hardening part of the model is expressed in form of a backstress tensor **a** that contains a 'recall'-term. The according backstress evolution law can be seen in equation (2). This rule is taken from the original Armstrong-Frederick model [2] and directs the movement of the yield surface through the principal stress space. The parameters C and γ are material parameters which can be obtained from cyclic test data.

2.2 Ductile crack imitation criterion and corresponding damage evolution law

During seismic events such as earthquakes the material impacting load can be characterized as ultra-low cyclic fatigue conditions, whereas the material can undergo only a few loading cycles with large plastic strains until it fails. It is therefore crucial to have an

accurate description of the damage initiation conditions and a damage evolution law that can reproduce the ongoing softening of the material in a precise manner. To represent these effects, damage is coupled to the plasticity model. The result is a hybrid plasticity and damage model based on the approach by Lian [1]. It is assumed the material shows pure plastic behavior before damage initiation. When damage initiates the material undergoes damage induced softening. To consider loading conditions under cyclic loading an amount of equivalent plastic strain is considered to initiate as well as advance ductile damage which is called an effective damage concept. Concurrently, the influence of the third invariant of the deviatoric stress tensor and the stress triaxiality is considered too at damage initiation and included into the description if the damage initiation locus. As damage emerges through the material it is assumed that the material eventually separates when it reaches a critical amount. Figure 1 schematically depicts the stress-strain behavior of the material with the above described hybrid plasticity-damage model.
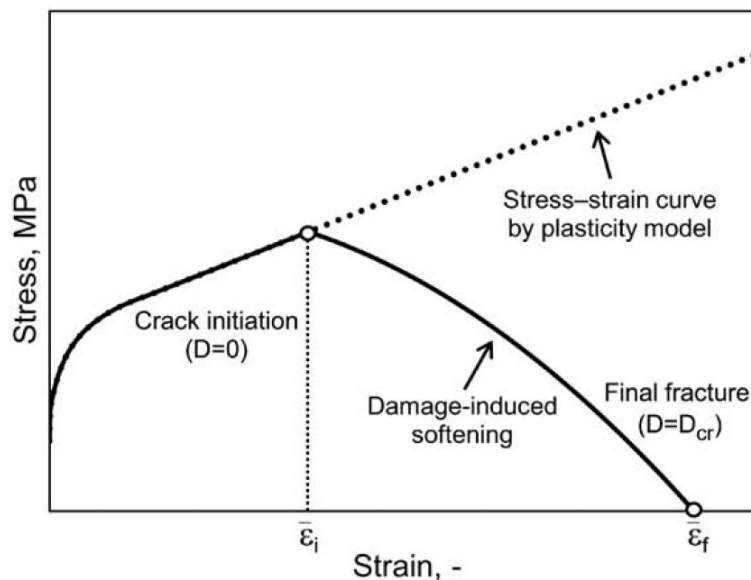
Figure 1: Schematic illustration of the stress-strain behavior with the hybrid plasticity and damage model [1]

It has been shown in many works that hydrostatic pressure and fracture strain correlate [9-11]. As hydrostatic pressure increases, fracture strain decreases. Especially, Bai and Wierzbicki investigated in their work the influence of the equivalent plastic strain on fracture. Whereat, they found a dependence of the equivalent plastic strain on the stress triaxiality and the lode angle which can be expressed in the third invariant of the deviatoric stress tensor. In Figure 2 a representation of both stress triaxiality and lode angle can be seen in principal stress space. Different lode angles and stress triaxialities can be achieved by a variation of testing specimens as it is shown in Figure 3. The result is a three dimensional fracture locus depending on equivalent strain, stress triaxiality and lode angle.

Additionally, resulting from the investigations of Lian [1] on the onset of damage, a three dimensional damage initiation locus which is also depending on equivalent strain, stress triaxiality and lode angle is employed. Its mathematical representation can be found in

Equation (3). Here, the parameters C_1, C_2, C_3 and C_4 are material parameters which can be identified through a variation of small scale tests with different geometries.
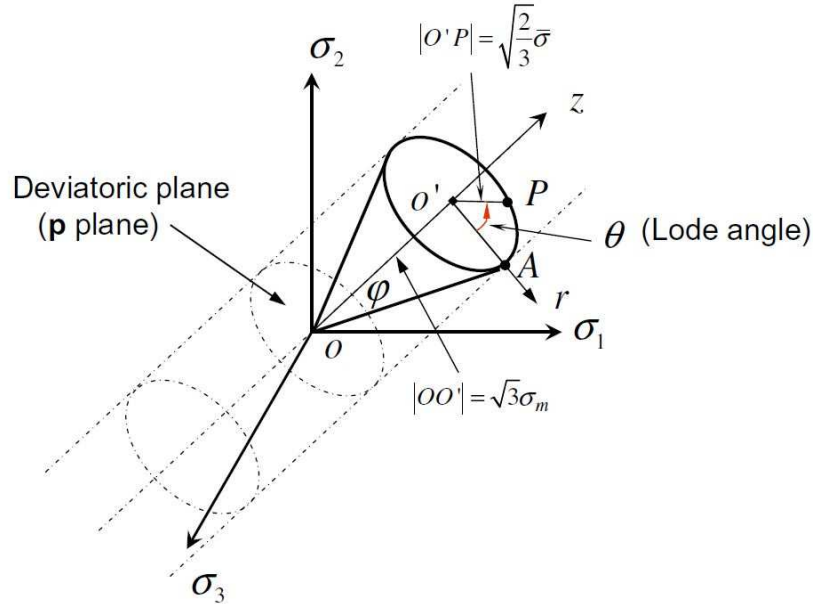

Figure 2: Geometric representation of a stress state in the mean stress space [3]
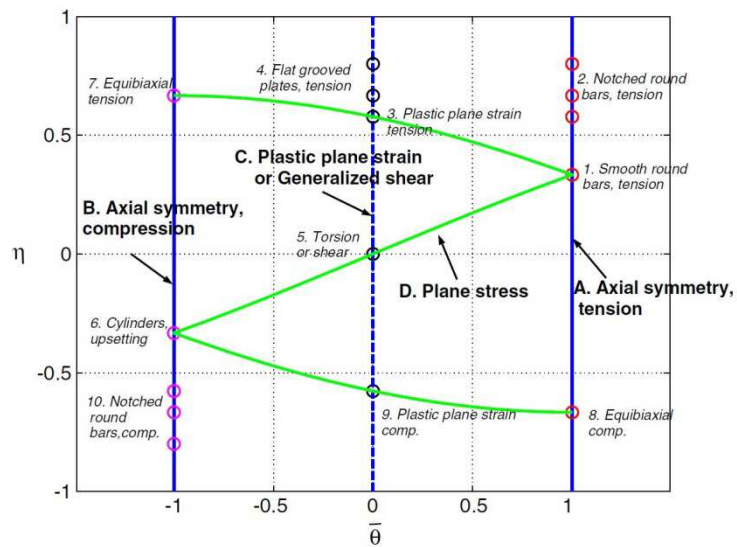

Figure 3: Representation of initial stress state [3]

Stress triaxiality η and lode angle parameter $\bar{\theta}$ can be obtained through Equations (4), repectively, (5).

$$\overline{\varepsilon}_i = (C_1 e^{-C_2 \eta} - C_3 e^{-C_4 \eta})\overline{\theta}^2 + C_3 e^{-C_4 \eta} \tag{3}$$

$$\eta = \frac{\sigma_m}{\overline{\sigma}} \tag{4}$$

$$\overline{\theta} = 1 - \frac{60}{\pi} = 1 - \frac{2}{\pi} arccos \left(\frac{\frac{27}{2} det([S])^{\frac{1}{3}}}{\overline{\sigma}} \right)^3 \tag{5}$$

Finally, an internal variable D is introduced to couple the ongoing damage induced material softening to the constitutive equations. Therefore the following damage evolution law is employed:

$$D_j = \begin{cases} 0; & \overline{\varepsilon}_{eff,j} \leq \overline{\varepsilon}_i \\ D_{j-1} + \frac{\sigma_{y0}}{G_f} \cdot \Delta \varepsilon_j \cdot \left(1 - e^{-m \cdot (D_{j-1}+0.1)} \right); & \overline{\varepsilon}_{eff,j} \geq \overline{\varepsilon}_i \wedge \overline{\varepsilon}_j < \varepsilon_f \wedge \eta_j > \eta_c \wedge m \neq 0 \\ D_{j-1} + \frac{\sigma_{y0}}{G_f} \cdot \Delta \varepsilon_j & \overline{\varepsilon}_{eff,j} \geq \overline{\varepsilon}_i \wedge \overline{\varepsilon}_j < \varepsilon_f \wedge \eta_j > \eta_c \wedge m = 0 \\ D_{cr}; & \overline{\varepsilon}_j = \varepsilon_f \end{cases} \tag{6}$$

It is assumed, to consider the cyclic loading conditions that an effective equivalent plastic strain ε_{eff} has to be reached in order to accumulate damage. This assumption is further formulated in Equations (7) and is based on the effective strain concept introduced by Ohata and Toyoda [4].

$$\Delta \varepsilon_{eff} = (1 - e^{-m \cdot \varepsilon_{eff}}) \cdot \Delta \varepsilon \tag{7}$$

Furthermore, the parameter G_f represents the dissipated energy for the crack opening at a unit area and the stress σ_{y0} equates the stress at damage initiation. Fracture occurs when a critical amount of damage D_{cr} is reached.

3 MATERIALS

In the following paragraph the investigated steel grades are characterized. The selected steel grades S500MC, S700, S355 with different toughness levels (T1) and (T2) were chosen to determine the damage initiation locus.

3.1 Chemical Composition

All presented steel grades were also micro alloyed. The chemical compositions (Table 1) were obtained by spectroscopic analysis.

**Table 1:** Chemical composition of the steel grades (in %)

S500MC	C	Si	Mn	P
	0.02	0.21	1.57	0.008

3.2 Microstructure

The microstructural analysis has been achieved by LOM. The microstructural composition can be found in Table 2. The corresponding pictures are shown in Figure 4.

**Table 2:** Microstructure analysis of the steel grades (in %)

Steel grade	Bainite	Pearlite	Ferrite
S500MC	100%	--	--
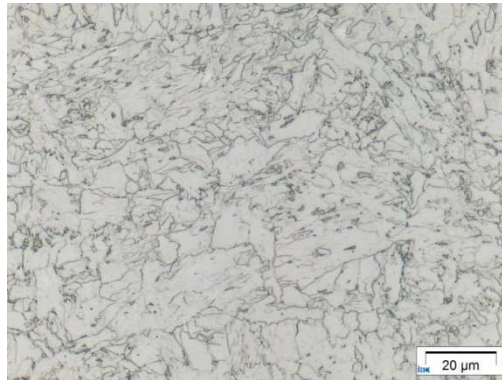
Figure 4: Microstructural configuration of (a) S500MC

3.3 Mechanical properties

Figure 5 shows the strength properties of the investigated steel grades. They have been achieved through tensile tests at room temperature. The extrapolation was done according to the Ludwik expression.
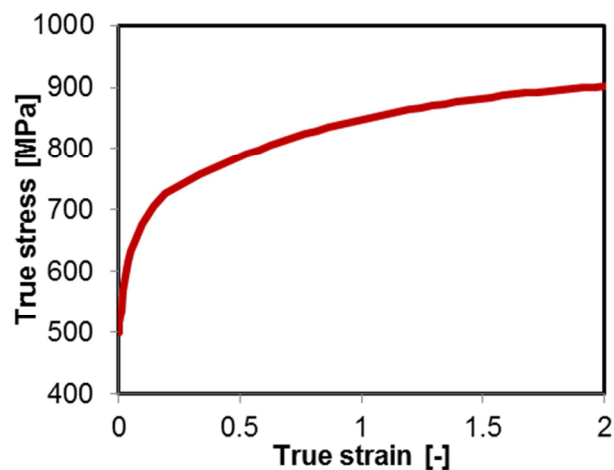
Figure 5: Flow curves of the selected steels S500MC

To consider temperature and strain rate effects on material behavior, equations (8) and (9) were employed and regarded for the materials' yield strength based on the approach by

Münstermann et al. [7]. The material parameters C_1^T, C_2^T and C_3^T to considers the temperature effect were obtained by tensile test at varying temperatures and are listed in Table 3.

$$f(T) = C_1^T \cdot \exp(C_2^T \cdot T) + C_3^T \tag{8}$$

Table 3: Calibrated parameters for temperature effect

	C_1^T	C_2^T	C_3^T
S500	0.0198	-0.018	0.983

The material parameter from Equation (9) $C_1^{\dot{\varepsilon}}$ and $C_2^{\dot{\varepsilon}}$ were obtained from high speed tensile tests and are listed in Table 4.

$$f(\dot{\varepsilon}) = C_1^{\dot{\varepsilon}} \cdot ln\dot{\bar{\varepsilon}}^p + C_2^{\dot{\varepsilon}} \tag{9}$$

Table 4: Calibrated parameters for strain rate effect

	$C_1^{\dot{\varepsilon}}$	$C_2^{\dot{\varepsilon}}$
S500	0.0023	1.0173

4   DETERMINATION OF DAMAGE INITIATION LOCUS

In order to obtain a toughness based safety assessment for a steel grade the determination the damage initiation locus (DIL) is crucial. The DIL indicates the beginning of the damage induced softening. The material specific DIL was obtained by calibrating the material parameters from Equation (3). Moreover, Equation (10) gives the critical damage variable D_{crit} before material failure and therefore the damage crack locus (DCL).

$$D_{crit} = \left(C_1^{crit}e^{-C_2^{crit}\eta} - C_3^{crit}e^{-C_4^{crit}\eta}\right)\overline{\theta} + C_3^{crit}e^{-C_4^{crit}\eta} + C_5^{crit} \tag{10}$$

The parameters were calibrated on a variation of small scale samples with different geometries, consequently, specimens with various stress states. The critical equivalent strain is estimated through the direct current potential drop (DCPD) method and later on then verified by metallographic investigations. For simulation Abaqus/Standard is used.

4.1 S500

For the construction steel S500, tensile tests with DCPD were conducted on notched round bar samples with different notch radii, on plane strain samples with different radii and on shear samples. According to the experimental results with DCPD method, the DIL can be determined, as shown Figure 6 (a).The tensile tests are simulated by Abaqus. The parameters D_3, G_f, and C_1^{crit} - C_5^{crit} are iteratively calibrated until the simulated force-displacement curves fit the experimental results, as shown exemplarily in Figure 7 for (a) a round bar

sample and (c) a shear sample. Accordingly the DCL of S500 is constructed and shown in Figure 6 (b). The calibrated parameter set for S500 is summarized in Table 5. To validate the calibrated parameters, those parameters are used in the simulation of Charpy test at room temperature. Figure 7 (b) shows the simulated force-displace curve of the Charpy test which corresponds to the experimental result.
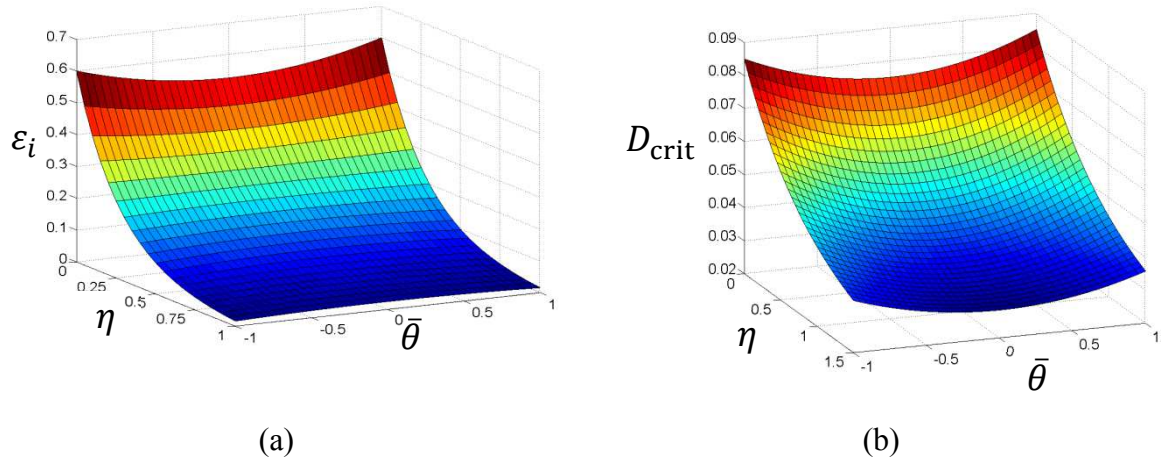

(a)   (b)

Figure 6: (a) DIL of S500 (b) DCL of S500

(a) RB   (b) Charpy test
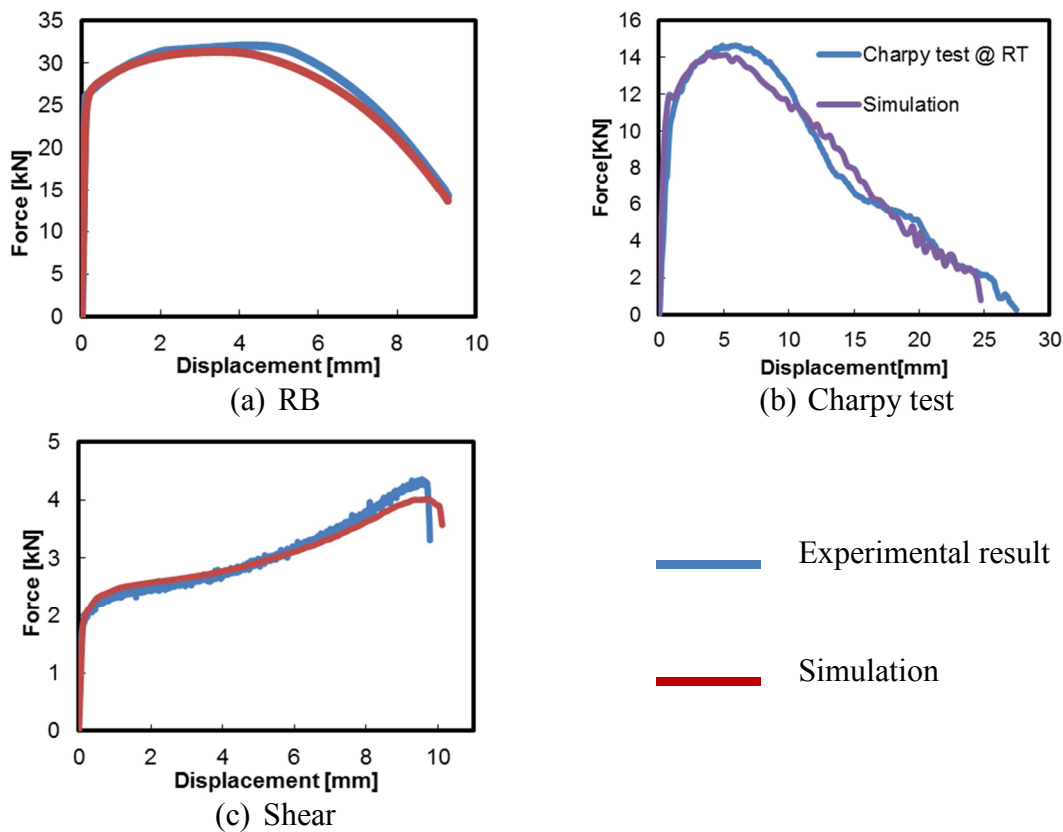
(c) Shear

Experimental result

Simulation

Figure 7: Force-displacement curves from tensile tests, Charpy tests and simulations (S500)

Table 5: Calibrated parameter set for S500

DIL				Damage evolution
C_1	C_2	C_3	C_4	G_f
0.6	3.644	0.5262	3.062	10000
DCL				
C_1^{crit}	C_2^{crit}	C_3^{crit}	C_4^{crit}	C_5^{crit}
0.06	0.895	0.05	1.415	0.025

5   DETERMINATION OF NOMINAL DUCTILE CRACK INITIAION LOCUS

The derivation of nominal ductile crack initiation loci stands on the nominal material properties, namely the nominal upper shelf toughness. To eliminate the chance of brittle fracture of steel components under operation, it is assumed that above 0 °C the steel toughness should be at upper shelf. According to EN 10025 [12], the required minimum impact energies corresponding the investigated steel grades are listed in Table 7.

Table 7: Minimum impact energy (longitudinal) according to delivery standard

Selected steel grade	Corresponding standard	20 °C	0 °C	-10 °C	-20 °C
S500ML	EN10025-4	63 J	55 J	51 J	47 J
S700	EN10025-6	--	50 J	--	40 J

To acquire the corresponding nominal upper shelf toughness, Wallin´s [13] approach is adapted. After Wallin, the Charpy transition curve of can be mathematically obtained from an exponential function as shown in Equation (13). The parameter C_{TC} controls the steepness of the transition curve.

$$C_{TC} \approx 34°C + \frac{\sigma_y}{35.1 MPa} - \frac{C_{V-US}}{14.3 J} \tag{13}$$

Through the Charpy impact energy the nominal ductile crack initiation loci is determined. The calibrated parameter sets are applied to Charpy test simulations. The computed impact energy as well as the load-deflection curve are compared to the experimental results at room temperature. Consequently, the DILs were fitted in order to match the computed impact energy to the previously determined nominal upper shelf toughness.

5.1 S500MC

By the multiplication of the factor for DIL and DCL, the computed Charpy impact energies are tailored to different target values. Figure 10**Fehler! Verweisquelle konnte nicht gefunden werden.** shows the obtained force-displacement curves and the corresponding nominal DIL for the target Charpy impact energies. Table 8 summarized the nominal DIL parameters for S500.
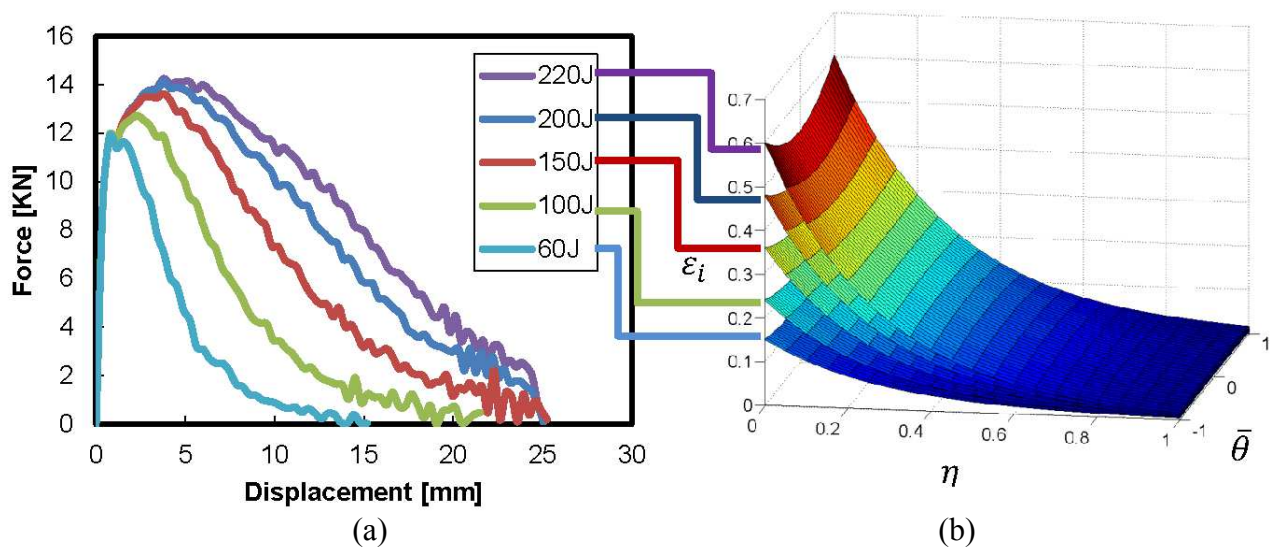
Figure 10: (a) Simulated force-displacement curves of Charpy tests with (b) varied DIL (S500)

Table 8: Nominal DIL for S500

Nominal Charpy impact energy	C_1	C_2	C_3	C_4
200 J	0.48	3.644	0.42096	3.062
150 J	0.36	3.644	0.31572	3.062
100 J	0.24	3.644	0.21048	3.062
60 J	0.144	3.644	0.13155	3.062

6   CONCLUSIONS

In the frame of this work, a coupled damage mechanics model for ULCF loading conditions was presented. It is based on the damage mechanics model by Lian and the plasticity model presented by Armstrong and Ferderick. Hereby, the focus was set on the determination of a crack initiation criterion and the following damage evolution restricted by an effective strain concept. This method was the applied to the construction steel S500. The damage initiation locus and the critical damage locus were obtained. Furthermore, a new criterion based on nominal toughness values was introduced to enable a prediction of the load capacity of the material according to the variation of toughness properties.

REFERENCES

[1]   J. Lian, M. Sharaf, F. Archie und S. Münstermann, „A hybrid approach for modelling of plasticity and failure behaviour of advanced high strength sheets," *International Journal of Damage Mechanics,* Nr. Vol. 22 (2), pp. 188-218, 2012.

[2]   P. Armstrong und C. Frederick, „A mathematical representation of the multiaxial Bauschinger effect," 1966.

[3] Y. Bai und T. Wierzbicki, „A new model of metal plasticity and fracture with pressure and Lode dependence," *International Journal of Plasticity,* Bd. 24, pp. 1071 - 1096, 2008.

[4] M. Ohata und M. Toyoda, „Damage concept for evalutating ductile cracking of steel structure subjected to large-scale cyclic straining," *Science and Technology of Advanced Materials,* Bd. 5, pp. 241-249, 2004.

[5] F. Yoshida und T. Uemori, „A model of large-strain cyclic plasticity describing the Bauschinger effect and workhardening stagnation," *International Journal of Plasticity,* Bd. 18, pp. 661 - 686, 2002.

[6] J. L. Chaboche, „On some modifications of kinematic hardening to improve the description of ratchetting effects," *Internatinal Journal of Plasticity,* Bd. 7, Nr. 7, pp. 661-678, 1991.

[7] S. Münstermann, C. Schruff, J. Lian, B. Dobereiner, V. Brinnel und B. Wu, „Predicting lower bound damage curves for high-strength low-alloy steels," *Fatigue & Fracture Eingineering Materials & Structures,* Bd. 36, pp. 779-794, 2013.

[8] A. L. Gurson, „Continuum Theory of Ductile Rupture by Void Nucleation and Growth: Part I—Yield Criteria and Flow Rules for Porous Ductile Media," *Journal of Engineering Materials and Technology,* Bd. 99, Nr. 1, pp. 2-14, 1977.

[9] G. Johnson und W. Cook, „Fracture characteristics of three metals subjected to various strains, strain rates, temperatures and pressures," *Engineering Fracture Mechanics,* Bd. 21, Nr. 1, pp. 31-48, 1985.

[10] J. Hancock und A. Mackenzie, „On the mechanisms of ductile failure in high-strength steels subjected to multi-axial stress-states," *Journal of the Mechanics and Physics of Solids,* Bd. 24, Nr. 2-3, pp. 147-160, 1976.

[11] F. McClintock, „A criterion of ductile fracture by the growth of holes," *Journal of Applied Mechanics,* Bd. 35, pp. 363-371, 1968.

[12] *EN 10025-2011: Hot rolled products of structural steels,* 2011.

[13] K. Wallin, Fracture Toughness of Engineering Materials: Estimation and Application, Warrington: EMAS Publishing, 2011.